Properties of pulsating solitons in dissipative systems

Wu Liang(吴 亮), Guo Zhi-Jie(郭志婕), and Song Li-Jun(宋丽军)†

College of Physics and Electronics Engineering and the State Key Subject of Optics, Shanxi University, Taiyuan 030006, *China*

(Received 23 November 2009; revised manuscript received 1 March 2010)

In this paper, a set of detailed numerical simulations of pulsating solitons in certain regions, where the pulsating solitons exist, have been carried out. The results show that the transformation between pulsating soliton and fronts can be realized through a series of period-doubling bifurcations, while there exist many kinds of special solutions. The complete transformation diagram has been obtained when the value of nonlinear gain varies within a definite range. The detailed analysis of the diagram reveals that the pulsating soliton experiences period-doubling bifurcations for smaller values of the nonlinear gain. For larger values of it, the pulsating solitons show chaotic behaviour and complex pulse splitting except for some special bifurcations. With the value of nonlinear gain increasing further, the pulse profiles resume pulsating, but the pulse energy is much higher than before and the pulse centre may move along the propagation direction.

Keywords: dissipative systems, pulsating soliton, bifurcation
PACC: 0545, 4265S

1. Introduction

Dissipative systems are more complicated than Hamiltonian ones because they include energy exchange with external sources. The generic equation which describes dissipative systems is the complex Ginzburg–Landau equation (CGLE),[1−3] which can be used to describe a vast variety of nonlinear phenomena in physics.[4−7] In particular, it describes a pulse generated by passively mode-locked lasers,[8,9] and signal transmission in all-optical communication lines.[10] The variety of these systems is enormous. Moreover, the number of solutions to this equation, even in the case of a cubic nonlinearity, is so large that the sphere of this knowledge by itself has been called "the world of the Ginzburg–Landau equation".[11,12]

Dissipative systems, in contrast to Hamiltonian ones, admit pulsating solitons. But the parameters of the CGLE must be far enough from the nonlinear Schrödinger equation (NLSE) limit in order to obtain pulsating solitons. An example of a pulsating soliton of the CGLE in the region of normal dispersion has been presented by Deissler and Brand.[13] In the years that followed, the pulsating solitons were studied in details.[12−16] In 2001, Akhmediev and his groups[14] presented the detailed existing regions of the three types of solitons, i.e. pulsating, erupting and creeping solitons, and studied the bifurcations within a definite parameter ranges. Afterwards, they presented the bifurcations of creeping soliton in detail.[12] A bifurcation diagram has been constructed for the region of transition between solitons and fronts, and various types of localized solutions have been presented. In fact, each of the three types of solitons has its own unattached existing parameter region, therefore the characteristics of them may be completely different.

Except the simulation solutions, some analytic expressions of CGLE solutions have been reported.[17−19] This problem is not simple as there are several parameters of the CGLE that define the region of existence for both stationary and pulsating solitons. Recently, Mancas presented a generalized variational formulation[17] to address the pulsating solitons without speeds and from that the periodic evolution of the trial function parameters to stable periodic attractors is derived, which agrees with the simulation results. However, except for the zero-velocity periodic pulsating solitons, CGLE also has non-zero velocity pulsating solitons, and the speed may be constant, periodic, quasi-periodic, or chaotic, although the quasi-periodic or chaotic speed has not been reported.

In this article, the detailed period bifurcation diagram of pulsating soltions has been obtained and some new solutions are also presented. The simulation results include a sequence of period-doubling bifurcations of pulsating solitons in the region of transition

†Corresponding author. E-mail: songlij@sxu.edu.cn
© 2010 Chinese Physical Society and IOP Publishing Ltd

between solitons and fronts, soliton bifurcation behaviours in chaotic region, and variation behaviours of the soliton specific structures. We have obtained not only the period-doubling bifurcation diagram, but also the moving and zero-velocity pulsating solitons as those in Ref. [12]. In particular, we have also found that the pulsating soliton can split and then the two or more parts combine into another periodic structure, which has not been presented before, for some special values of nonlinear gain. Furthermore, the bifurcations in the chaotic region have also been presented when the nonlinear gain is located in some very small region.

2. Complex Ginzburg–Landau equation and numerical simulations

The cubic-quintic complex Ginzburg–Landau equation (CGLE) is a general model for dissipative systems, in dimensionless form, the CGLE can be written as[12−16]

$$\begin{aligned} &\mathrm{i}\,\psi_z + \frac{D}{2}\psi_{xx} + |\psi|^2\psi + \nu\,|\psi|^4\psi \\ &= \mathrm{i}\,\delta\psi + \mathrm{i}\,\varepsilon\,|\psi|^2\psi + \mathrm{i}\,\beta\psi_{xx} + \mathrm{i}\,\mu\,|\psi|^4\psi, \end{aligned} \tag{1}$$

where z and x are the propagation distance and time variable, respectively, and ψ is the normalized envelope of the field. D is the dispersion coefficient, with $D = \pm 1$, depending on whether the dispersion is anomalous or normal; δ is the linear gain-loss coefficient, β accounts for the spectral filtering, ε represents the nonlinear gain, μ characterizes the saturation of the nonlinear gain, and ν is the coefficient of the quintic nonlinearity.

The CGLE admits a variety of localized pulsating solutions, as well as period-doubling bifurcations.[12−14] In order to investigate soliton bifurcations in a finite region bound by a set of parameters, we have solved Eq. (1) using a split-step Fourier method. In most simulations, we use a numerical grid of 2048 points in x direction and a step size $\Delta z = 0.005$. The transmission distance is $z = 5000$. In some critical regions we choose a numerical grid of 4096 points (or even more) and longer propagation distance in z direction because it is important for the results to obtain the true approximated solutions of CGLE.

In order to investigate the pulsating soliton periodicity and bifurcation, we fix the parameters as $D = +1$, $\nu = -0.08$, $\delta = -0.1$, $\beta = 0.05$, $\mu = -0.1$ except for the nonlinear gain. Then we change slightly the parameter ε to study the behaviours of the solution. When the value of nonlinear gain ε is given, the definite solution is evolved after a certain distance of transmission. The region of parameter ε from 0.7 to 0.8 has been analysed in detail and the maximal values of the soliton energy have been found, as shown in Fig. 1. Since the minima of Q show much smaller fluctuations than the corresponding maxima, only the maxima of Q for pulsating solitons are given in Fig. 1. From the figure, we can see that the pulsating soliton bifurcations occur more than once with the variation of ε, as framed by dashed line rectangle in Fig. 1. And the solutions show chaotic motion firstly when the nonlinear gain parameter ε is equal to 0.7277. The chaotic motion represents that the solutions are pulsations but without periodicity, so their maximal energies vary randomly, as marked by the black regions in the figure. But when the parameter ε is larger than 0.7828, the solution resumes periodical pulsations again. At the same time, with increasing ε, the first zero-velocity pulsating soliton will transform into moving solution, as labeled with letter J in Fig. 1. When the ε is larger than 0.761, the pulse split is observed for the first time. The maximum values of soliton energy are larger than that for smaller ε and vary randomly, so the black region filled the whole window in Fig. 1. The behaviours of soliton within this region are very complex and need further work to analyse them later. The gray region in Fig. 1 shows that the front solutions is evolved when ε is larger than 0.7887. In the following sections, we shall present a detailed description of each of these different types of solutions.

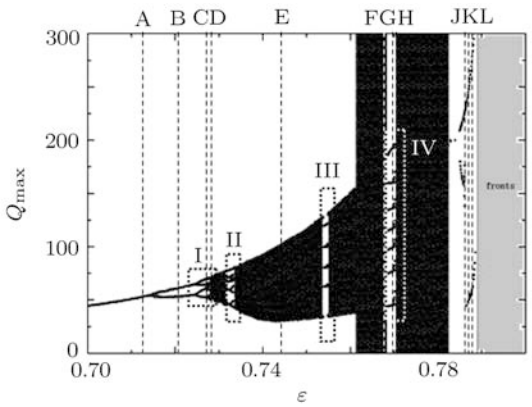


Fig. 1. Soliton energy bifurcation diagram for varying ε. The rest parameters are fixed: $D = 1$, $\delta = -0.1$, $\beta = 0.05$, $\mu = -0.1$, and $\nu = -0.08$.

3. Period-doubling bifurcations of pulsating solitons

In the nonlinear systems, period-doubling bifurcations have been discussed as an important subject in the literature. In optics, period-doubling bifurcations have been found experimentally in various laser systems. These include semiconductor lasers,[20] femtosecond solid-state lasers,[21] F-centre lasers,[22,23] fibre lasers,[24,25] nonlinear cavities,[26,27] and gaseous lasers.[28] Period-doubling in terms of a train of pulses has been observed in mode-locked lasers and nonlinear fibre ring resonators.

Figure 1 shows clearly a variety of qualitatively different behaviours, which are labeled with letters from A to L at the top of the diagram. And we can see that the first bifurcation occurs at $\varepsilon = 0.715$, where one-period pulsating solution bifurcates to double-period pulsations. When the value of parameter ε is smaller than 0.715, the soliton changes its shape periodically in the z direction and one pulsation makes one period, as shown in Fig. 2(a), the pulse profile for $\varepsilon = 0.712$. When the parameter ε changes from 0.7 to 0.714, the solution always presents a single periodic pulsating soliton. As the value of ε is increased high enough, the period of pulsating soliton doubles, that is, the profile repeats itself after two pulsations, as shown in Fig. 2(b). For comparison, the energy evolution diagrams of them are shown in Fig. 3, from which the pulsating properties of one-period and double-period can be seen clearly. For larger values of parameter ε, 4-period and 8-period pulsations can also be obtained, as shown in Fig. 4 the magnified graph of part I, which is framed by dashed line in Fig. 1. The corresponding profiles of 4-period and 8-period pulsations are shown in Fig. 5, as labeled with C and D in Fig. 1 and Fig. 4, respectively.

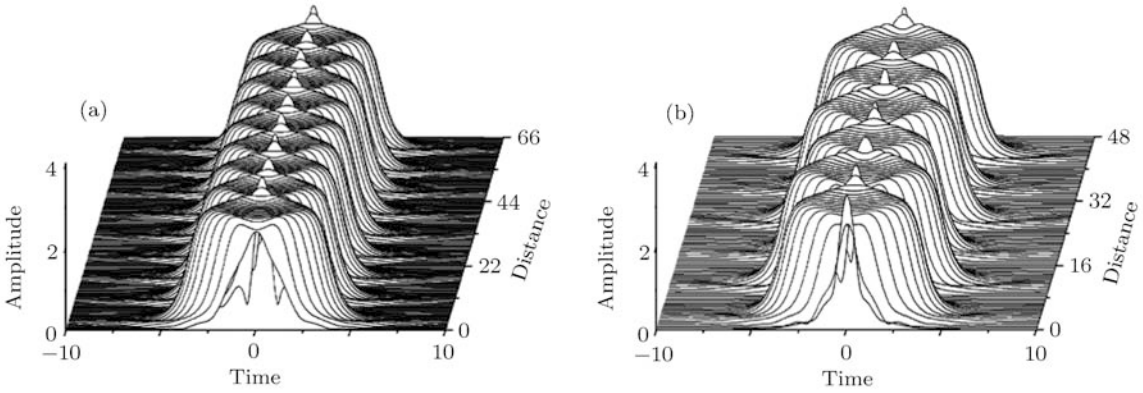


Fig. 2. Pulsating solitons at (a) $\varepsilon = 0.712$ and (b) $\varepsilon = 0.72$, respectively, the other parameters are the same as those in Fig. 1. (lines A and B in Fig. 1).

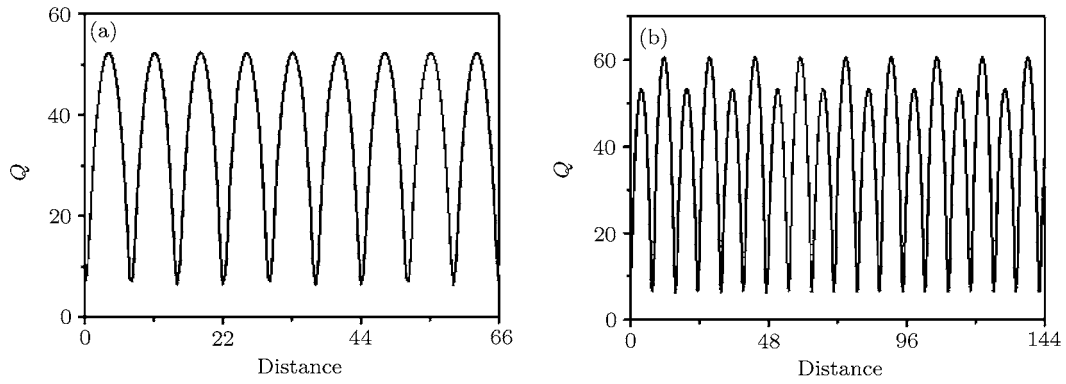


Fig. 3. Soliton energy diagrams at (a) $\varepsilon = 0.712$ and (b) $\varepsilon = 0.72$.

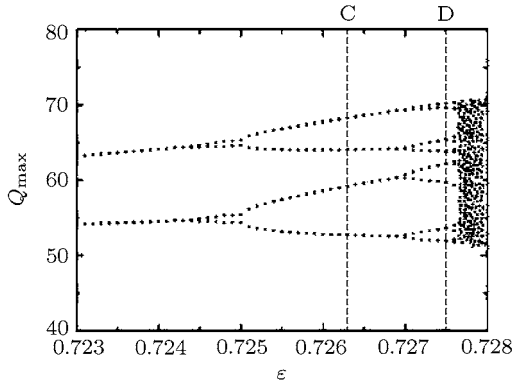


Fig. 4. Magnified region of the bifurcation diagram, shown as the dashed square I in Fig. 1.

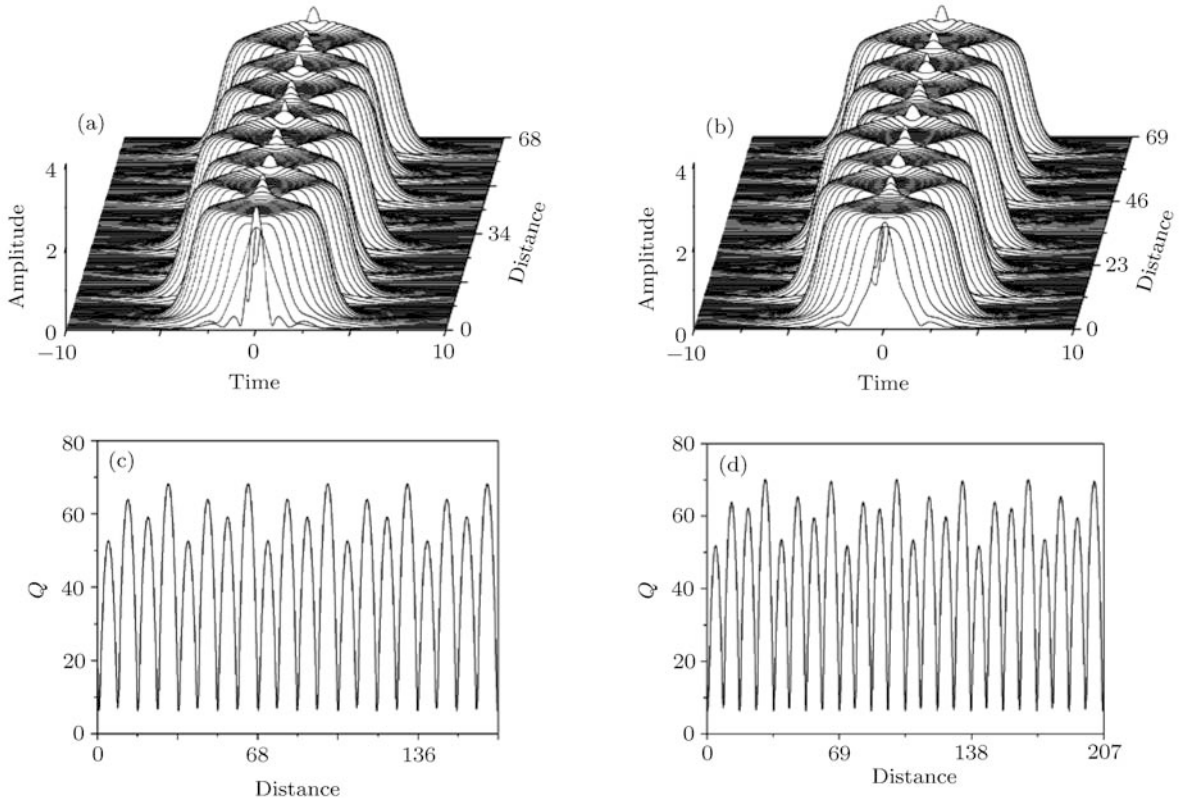


Fig. 5. Pulsating solitons at (a) and (c) $\varepsilon = 0.7263$, (b) and (d) $\varepsilon = 0.7275$, the other parameters are the same as those in Fig. 1 (lines C and D in Figs. 1 and 4).

4. Soliton splitting behaviours and special bifurcations in chaotic region

When the value of ε is larger than 0.7277, the pulse shape does not repeat itself in each (or several) pulsation(s) and the evolution is chaotic. But the maximum value of Q almost varies within a definite range when the nonlinear gain ε is smaller than 0.761. For example, the maximum value of soliton energy is restricted within the range from 30 to 98.5 when the value of nonlinear gain is equal to 0.743, which are shown in the contour plot and the energy diagram in Fig. 6.

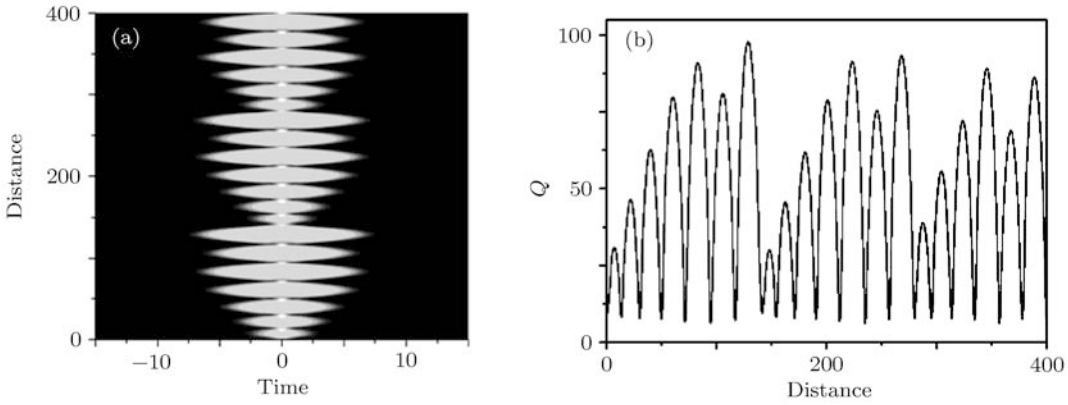


Fig. 6. (a) Contour plot and (b) the maximum energy for $\varepsilon = 0.743$ (line E in Fig. 1).

Further increase of the value of ε, up to near the region labeled IV in Fig. 1, the solutions become unstable so that the pulse profiles change chaotically as they evolve. The chaotic motion frequently splits the pulse into two or even more parts, which may transmit separately or combine into one. For each soliton, the range of allowed Q values is limited, but the process of their multiplication widens this range to infinity. There are no regular scenarios of soliton evolution in this range. An example of chaotic evolution of the soliton profile, where there are three solitons in the numerical window, is shown in Fig. 7(a). Each soliton remains localized unless it merges with another one or splits into two new solitons. An example of the latter process is shown in Fig. 7(b).

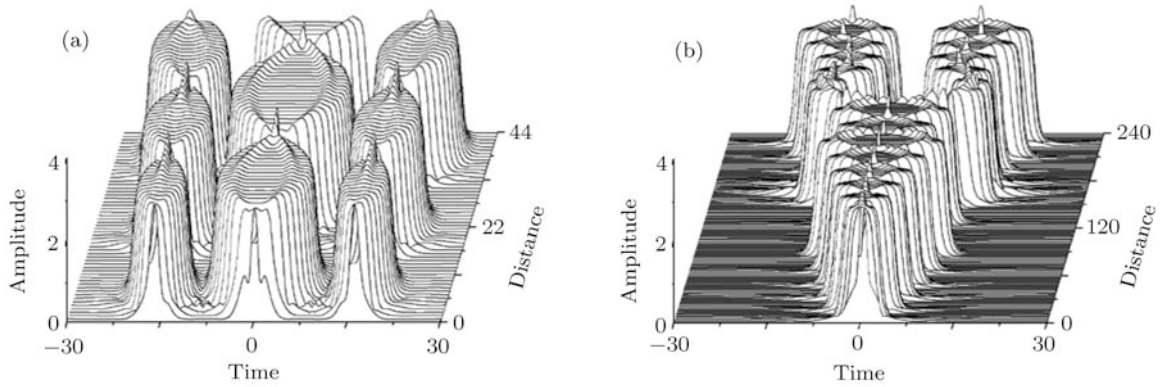


Fig. 7. (a) Typical propagation profile at $\varepsilon = 0.767$ (line F in Fig. 1). (b) Solitons at this value of ε are unstable and may split into two solitons.

The average distance that each soliton travels before splitting or interacting with another one depends on ε and the density of solitons already existing in the numerical window. These phenomena are similar to those in Ref. [12].

Furthermore, there are several special bifurcations that emerge in the chaotic region, which seem to have no relations with the bifurcations that occurred before. The first bifurcation occurs when the nonlinear gain ε is equal to 0.7326 and is beginning with 5-period, but not even periods. Figure 8(a) is the magnified plot of part II, which is framed by dashed lines in Fig. 1. The second bifurcation is located at $\varepsilon \in [0.754, 0.7548]$ and starts with 4-period, as shown in Fig. 8(b). After twice bifurcating, we can obtain 16-period pulsating solitons within this region. The third bifurcation is very different from the above two, it has not only pulsating, but also splitting along the transmission path. When the value of nonlinear gain is larger than 0.7687 but smaller than 0.7702, the pulse may split into another two pulses and then combine into one pulse or keep two separated pulses. And the periodical characteristics after splitting are also different for different values of the nonlinear gain. For example, when the nonlinear gain $\varepsilon = 0.7696$, the splitting occurs after a certain distance of chaotic evolution and then the two pulsating solitons keep transmitting separately and periodically, as shown in Fig. 9(a), the contour plot within $z = 1500$. For clarity, we plot the detailed behaviour of the two periods

in Figs. 9(c) and 9(e), which are three-dimensional (3D) plot and the maximum value curve of soliton energy, respectively.

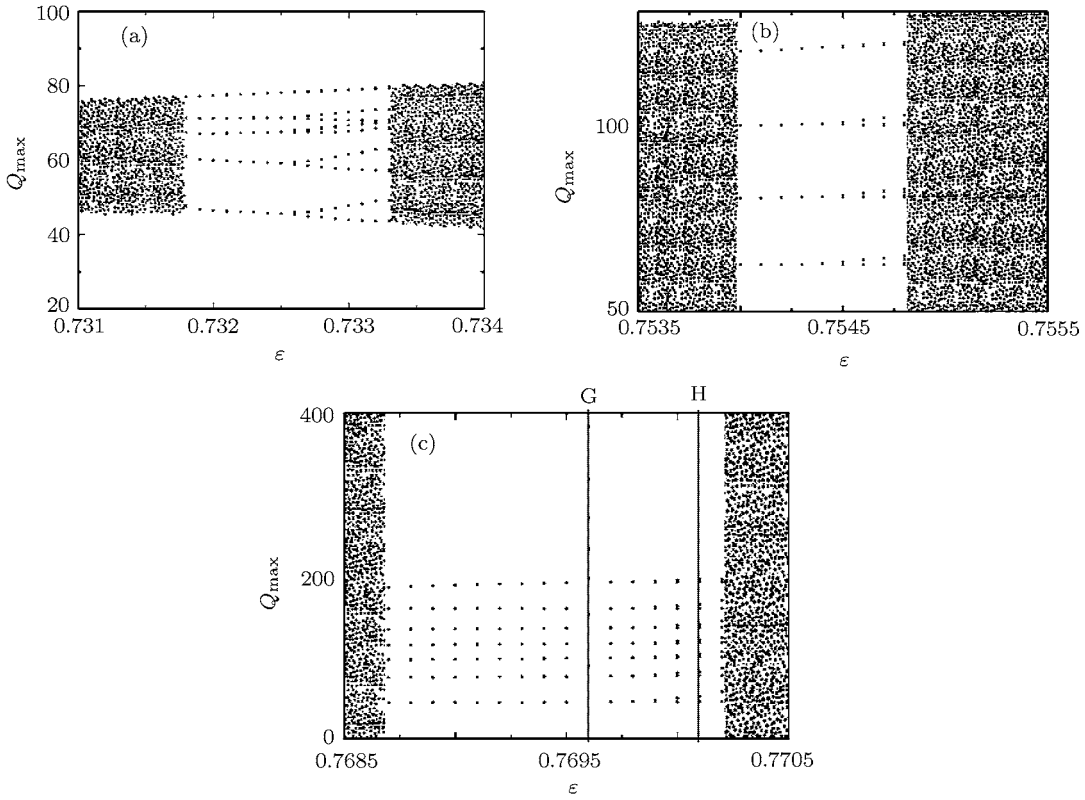
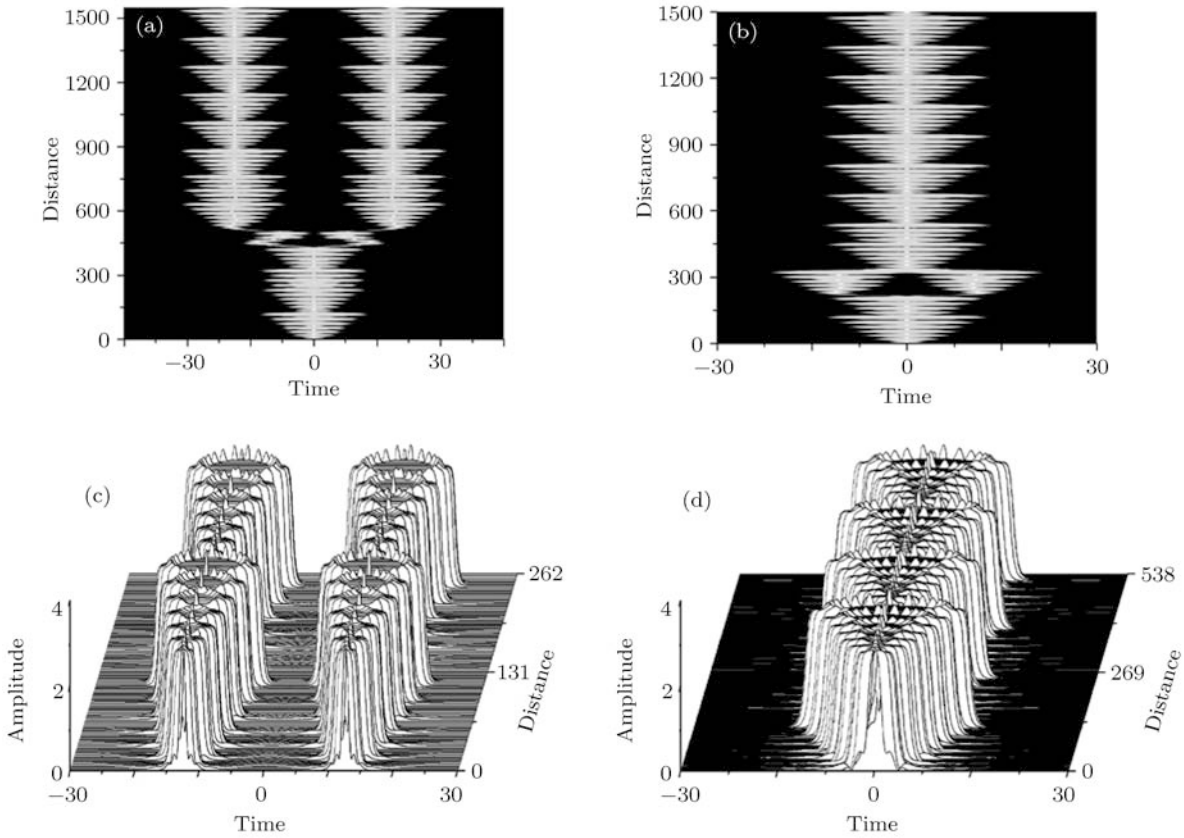


Fig. 8. Magnified regions of parts (a) II, (b) III, and (c) IV framed by dashed lines in Fig. 1.



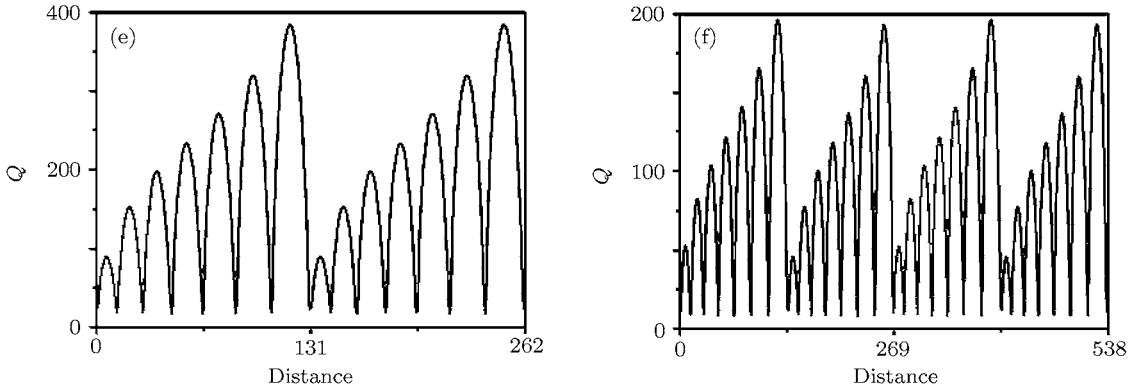


Fig. 9. (a) Contour plot, (c) propagation profile and (e) the maximum energy for $\varepsilon = 0.7696$; (b), (d) and (f) the corresponding plots for $\varepsilon = 0.7701$ (lines G and H in Figs. 1 and 8).

It is surprising that these two pulsating solitons are also 7-period, but the maximum values of Q are almost twice as large as those for $\varepsilon = 0.7695$. But when $\varepsilon = 0.7701$, the splitting also occurs after a certain distance of evolution. Then the two pulsating solitons unite into one pulse which keeps periodically evolving, as shown in Fig. 9(b), the contour plot within the same transmission distance. The corresponding 3D plot and the maximum value curve of soliton energy are shown in Figs. 9(d) and 9(f), indicating that the soliton is 14-period, and the maximum value of energy is not so high as shown in Fig. 9(e). For clarity, only two periods are plotted in Figs. 9(c)–9(f). A lot of numerical simulations show that the same behaviour, which is first split and then unite into one, can be obtained for other values of ε. The only difference between them may be their periodicity.

5. Multiplicity of solutions

In this section, we concentrate on the range of parameters that are in the transition region between pulsating solitons and front solutions, which is relatively narrow in comparison with the whole region of pulsating solitons. This transition is far from being a trivial phenomenon like a simple increase of the soliton width. As a consequence, it is a very dense region with various types of soliton solutions, such as zero-velocity, non-zero velocity or varied velocity pulsating soliton and non-zero velocity localized solutions, etc. Magnification of this region is shown in Fig. 10, in which more than one solution exist for the same value of the nonlinear gain, such as for $\varepsilon = 0.7861$ the initial pulse first converges to zero-velocity pulsating soliton, but later transforms into non-zero velocity pulsating soliton due to the instability of soliton with zero-velocity. The two kinds of soliton and the process of transformation are shown in Fig. 11. The branch of solutions with the label of moving pulse (MP) exists from $\varepsilon = 0.7851$ up to 0.7862, which also can be found in Ref. [12]. In this branch, there is another solution with lower energy which is denoted as composite pulse (CP). This type of solution has a bump in the central part and two fronts located symmetrically on each side of the pulse. The central symmetry of the soliton profile results in its zero velocity. The profile of CP solution is shown in Fig. 12, from which we can see that the pulse centre has no velocity along the transmission direction. The localized solutions with chaotic velocities have also been found for some definite values of nonlinear gain, such as $\varepsilon = 0.7867$ in Fig. 13. The transformation of first zero-velocity pulsating soliton to the moving localized pulse is shown in Fig. 14(a) and the profile of this localized pulse is presented in Fig. 14(b), which almost keeps its shape without pulsating.

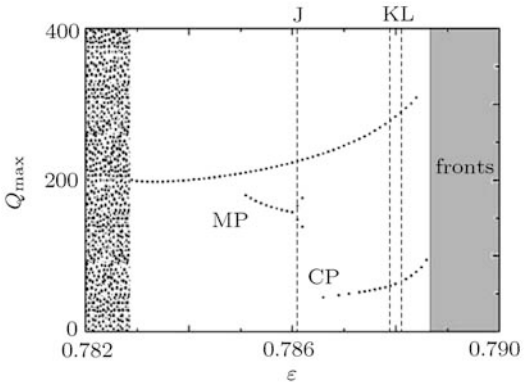


Fig. 10. The enlarged region between pulsating solitons and front solutions.

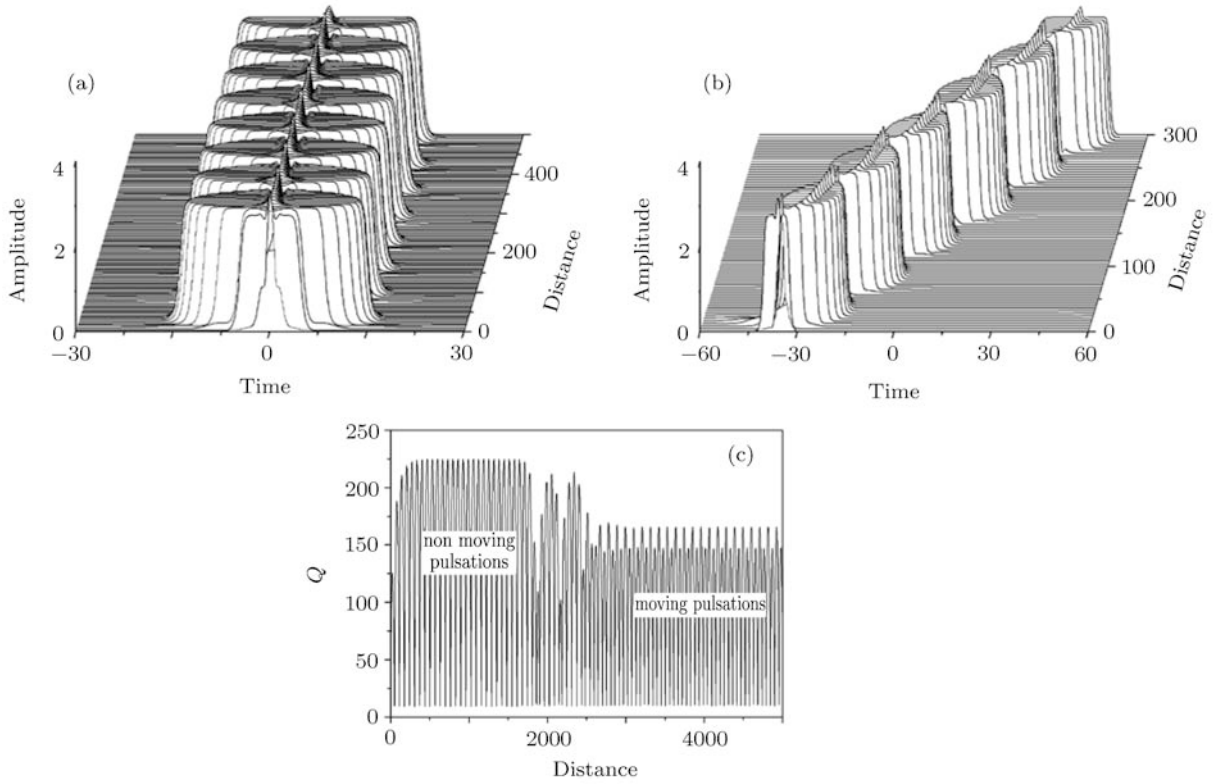


Fig. 11. (a) Zero-velocity pulsating soliton, (b) pulsating soliton with a definite velocity, and (c) energy versus propagation distance for $\varepsilon = 0.7861$, (line J in Figs. 1 and 10).

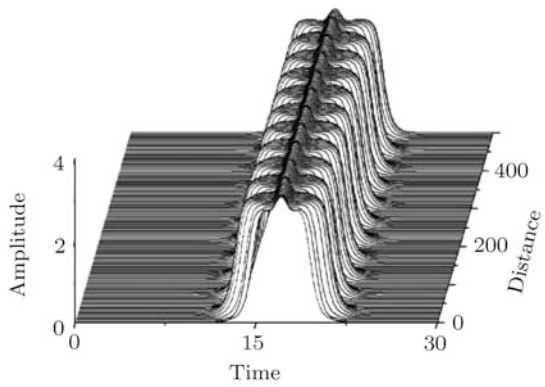


Fig. 12. Propagation profile for $\varepsilon = 0.7879$, (line K in Figs. 1 and 10).

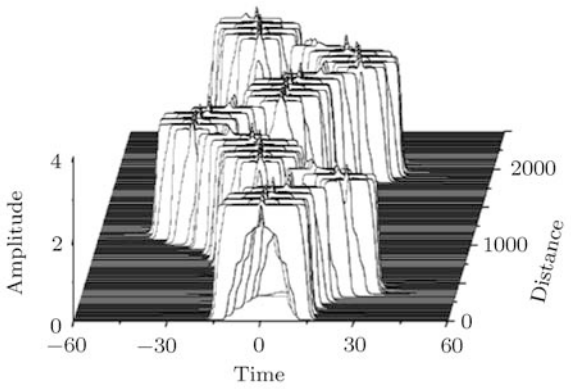


Fig. 13. Propagation profile for $\varepsilon = 0.7867$.

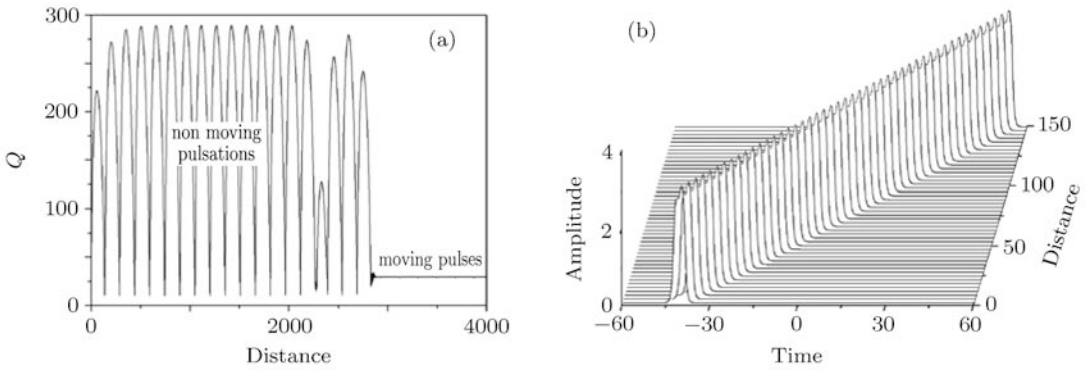


Fig. 14. (a) Energy versus propagation distance, and (b) localised solution with a definite velocity for 0.7881 (line L in Figs. 1 and 10).

Furthermore, we have also studied the stability of the solutions. We have carried out numerical evolutions of initial optical pulses under the influence of some white noise and the results show that the solutions are stable under the disturbance of a definite range of noises. For example, when the value of the nonlinear gain is equal to 0.7275, the initial pulse can also converge to 8-period pulsating solitons for the maximum value of white noise 0.1, as shown in Fig. 15.

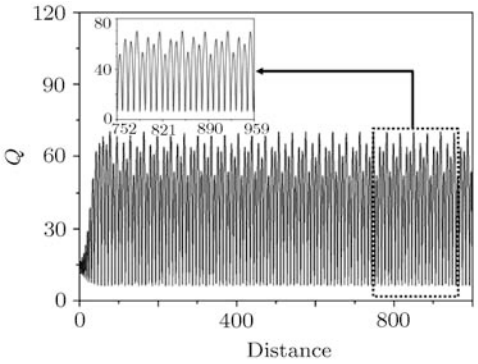


Fig. 15. Evolution of the initial pulse under some white noise for $\varepsilon = 0.7275$; the maximum value of white noise is 0.1.

From the figure, we can see that the 8-period pulsating solitons converge after moving a distance and the period is the same as that without white noise. The inset shows the detailed periods, which are framed by dotted lines in Fig. 15 and the same as that without noise in Fig. 5(d).

6. Conclusion

In conclusion, a set of detailed numerical simulations of pulsating solitons in the existing regions have been carried out. The results show that the transformation between pulsating soliton and fronts is not realized only through a series of period-doubling bifurcations, but also contains many kinds of special solutions. The complete transformation diagram has been obtained for a definite range of the nonlinear gain values. The detailed analysis of the diagram reveals that the pulsating solitons experience the period-doubling bifurcations for smaller values of the nonlinear gain. For larger values, the pulsating solitons show chaotic behaviour and complex pulse splitting except some special bifurcations. With the value of nonlinear gain increasing further, the pulse profiles resume pulsating, but the pulse energy is much higher than before and the pulse centre may vary with the transmission distance.

References

[1] Normand C and Pomeau Y 1977 *Rev. Mod. Phys.* **49** 581
[2] Kuramoto Y 1984 *Chemical Oscillations, Waves and Turbulence* (Berlin: Springer-Verlag)
[3] Zheng L and Tang Y 2010 *Chin. Phys.* B **19** 044209
[4] Lei S L and Wu H S 1965 *Acta Phys. Sin.* **21** 1355 (in Chinese)
[5] Wang K G 1993 *Acta Phys. Sin.* **42** 256 (in Chinese)
[6] Ding W S, Liu L H and Xi L 2008 *Acta Phys. Sin.* **57** 7705 (in Chinese)
[7] Liang C H and Tan K B 2007 *Acta Phys. Sin.* **56** 2704 (in Chinese)
[8] Moores J D 1993 *Opt. Commun.* **96** 65
[9] Soto-Crespo J M, Akhmediev N and Ankiewicz A 2000 *Phys. Rev. Lett.* **85** 2937
[10] Mollenauer L F, Gordon J P and Evangelides S G 1992 *Opt. Lett.* **17** 1575
[11] Aranson I S and Kramer L 2002 *Rev. Mod. Phys.* **74** 99
[12] Chang W, Ankiewicz A, Akhmediev N and Soto-Crespo J M 2007 *Phys. Rev.* E **76** 016607
[13] Deissler R J and Brand H R 1994 *Phys. Rev. Lett.* **72** 478
[14] Akhmediev N, Soto-Crespo J M and Town G 2001 *Phys. Rev.* E **63** 056602
[15] Tian H P, Li Z H, Tian J P, Zhou G H and Zi J 2004 *Appl. Phys.* B **78** 199
[16] Song L J, Li L and Zhou G S 2007 *Chin. Phys.* **16** 148
[17] Mancas S C and Choudhury S R 2009 *Chaos, Solitons and Fractals* **40** 91
[18] Mancas S C and Choudhury S R 2007 *Theor. Math. Phys.* **152** 1160
[19] Tsoy E N and Akhmediev N 2005 *Phys. Lett.* A **343** 417
[20] Carpintero G and Lamela H 1997 *J. Appl. Phys.* **82** 2766
[21] Cote D and van Driel H M 1998 *Opt. Lett.* **23** 715
[22] Sucha G, Bolton S R, Weiss S and Chemla D S 1995 *Opt. Lett.* **20** 1795
[23] Sucha G, Chemla D S and Bolton S R 1998 *J. Opt. Soc. Am.* B **15** 2847
[24] Luo L G, Tee T J and Chu P L 1998 *J. Opt. Soc. Am.* B **15** 972
[25] Coen S, Haelterman M, Emplit Ph, Delage L, Simohamed L M and Reynaud F 1998 *J. Opt. Soc. Am.* B **15** 2283
[26] Haelterman M 1992 *Appl. Phys. Lett.* **61** 2756
[27] Boyce J and Chiao R Y 1999 *Phys. Rev.* A **59** 3953
[28] Chizhevsky V N and Corbalan R 1996 *Phys. Rev.* E **53** 1830